Design and Control of a Modular Multilevel DC/DC Converter for Regenerative Applications

Daniel Montesinos-Miracle, *Senior Member, IEEE*, Miquel Massot-Campos, Joan Bergas-Jané, *Senior Member, IEEE*, Samuel Galceran-Arellano, and Alfred Rufer, *Fellow, IEEE*

***Abstract*—This paper compares different cascaded and multilevel topologies to interface supercapacitors to a dc bus in regenerative braking applications. It is shown that the modular multilevel dc/dc converter (MMC) can benefit from both reduced voltage and increased frequency across the inductor to reduce its weight and volume when using phase shifting modulation. The proposed control method is able to balance supercapacitor voltage while providing precise output current control. The converter topology and control method are validated with simulations and experimental results.**

***Index Terms*—Control strategies, modular multilevel converters (MMCs), phase shifting, supercapacitors (SCs).**

I. Introduction

REGENERATIVE braking is not only present in electric vehicle (EV) or hybrid vehicle [1]. Many electric traction applications such as elevators [2], [3] and railway [4] can also benefit from regenerative braking. The braking energy can be dissipated in resistors or stored in different systems such as batteries, capacitors, flywheels, or superconductive magnets [5], but for simplicity and for its high power capability, supercapacitors (SCs) are preferred in front of others [1], [6].

SCs are energy storage devices that do not have mobile parts, and they storage energy in the form of electric field. SCs are stated as power sources, in front of batteries that are used as energy sources. So they are best placed in applications where high power levels are needed during a short period of time, from milliseconds to few hundreds of seconds. Utility applications include uninterruptible power systems or utility voltage stabilizers in wind farms or photovoltaic (PV) plants. Regenerative braking in any type of mobility application (hybrid and EV cars, trams, buses, cranes, and fork lifts) is one of the main applications. They can fit also in heavy diesel engines as a power sources when starting or in start/stop applications.

In mobile applications, SCs are often paired with batteries [7] in order not to degrade their life, to increase efficiency, and to provide instant power whenever it is demanded. In these applications, SCs provide constant power and batteries' constant energy [8].

However, direct parallelization of SC and batteries has many drawbacks. There is no control on where the energy is flowing from or to and also the voltage at which the capacitors are connected is almost constant. Therefore, SCs are not used as an energy source but as a powerful decoupling capacitor, which is not what it is intended for. To achieve energy management capabilities, a converter has to be placed to control the energy flow in an SC [8].

SCs are low-voltage devices. To achieve the high voltage needed in traction applications, a large number of cells have to be connected in series. This series connection can cause voltage imbalances due to the difference in capacitance of each SC cell because of common series current. These imbalances could cause premature failure of the SC or even destruction of cells. Passive and active power electronics-based devices have been proposed in the literature for cell voltage balancing [9], [10]. Commercially available SC banks reach voltages up to 200 V [11], but active voltage-balancing methods must be used.

Another possible way to limit the number of series-connected cells is to parallel them. But then, some voltage adaptation must be used in order to connect the SC to the high-voltage dc bus. Voltage adaptation can be achieved using bidirectional boost converter, but a large inductor is needed. Using multichannel interleaved converters, the size of inductor can be reduced and efficiency can be increased if the discontinuous conduction mode is used [12]–[15]. DC/DC bidirectional transformer isolated converters are also used [2].

To obtain high voltage from low-voltage devices, or vice versa, cascaded and multilevel converters have been employed in the literature [16]. In [17], dc/dc converters are cascaded to obtain higher bus voltage in PV applications. Vorperian [18] used forward converters in a 10 kV to 400 V converter. Series–parallel connection of converters is of interest in low-voltage high-current applications such as computer and telecommunications power supplies [19], [20] to increase reliability, efficiency, and standardization. In [21], a modular multilevel converter (MMC) is used as a traction converter in an hybrid vehicle achieving charge balance in batteries. The use of MMCs is a

Manuscript received July 30, 2012; revised October 4, 2012; accepted November 21, 2012. Date of current version January 18, 2013. Recommended for publication by Associate Editor Prof. J. Choi.

D. Montesinos-Miracle, J. Bergas-Jané, and S. Galceran-Arellano are with the Centre d'Innovació Tecnològica en Convertidors Estàtics i Accionaments, Departament d'Enginyeria Elèctrica, Escola Teècnica Superior d'Enginyeria Industrial de Barcelona, Universitat Politècnica de Catalunya, 08028 Barcelona, Spain (e-mail: montesinos@citcea.upc.edu; bergas@citcea.upc.edu; galceran@citcea.upc.edu).

M. Massot-Campos was with the Centre d'Innovació Tecnològica en Convertidors Estàtics i Accionaments, Departament d'Enginyeria Elèctrica, Escola Tècnica Superior d'Enginyeria Industrial de Barcelona, Universitat Politècnica de Catalunya, 08028 Barcelona, Spain. He is now with Robotics and Vision Group, Balearic Islands University, 07122 Palma de Mallorca, Spain (e-mail: miquel.massot@gmail.com).

A. Rufer is with Industrial Electronics Laboratory, Ecole Polytechnique Fédéral de Lausanne, Lausanne CH-1015, Switzerland (e-mail:alfred.rufer@epfl.ch).

Digital Object Identifier 10.1109/TPEL.2012.2231702

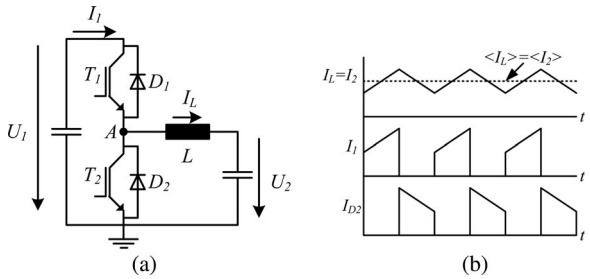

Fig. 1. Topology and typical current waveforms for an HB converter. (a) Topology of the HB converter connecting two voltage sources. (b) Typical current waveforms for an HB converter.

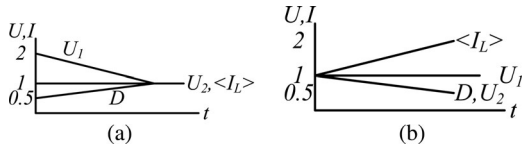

Fig. 2. Evolution of the voltages and duty cycle for the given converters when discharging the SCs. (a) Buck-mode converter. (b) Boost-mode converter.

good tradeoff between complexity and reliability [22]. Redundancy and control allow these converters to achieve more than one goal within the imposed control scheme.

This paper presents the design and the control of a modular multilevel dc/dc converter intended to interface an SC bank and a high-voltage dc bus. The paper compares three proposed topologies based on the half-bridge (HB) converter in terms of the energy stored in its inductive components. The modular multilevel dc/dc converter will show higher performance, because it benefits from reduced applied inductor voltage and increased frequency, reducing inductor size for the same allowable inductor current ripple.

The paper also proposes a control method to equalize the energy stored in the SCs. Simulations and experimental results are used to validate the design and the control method proposed.

II. Cascaded and MMCs

Two quadrant dc/dc converter is needed in regenerative applications with energy storage in SCs. When braking, the energy flows into SCs, but when in the traction mode, the energy flows from SCs to the load. All the converters presented in this paper are based on the HB topology shown in Fig. 1(a). Some authors propose the cascaded connection of multilevel neutral point clamped or flying capacitor converter to achieve higher number of levels at the output [23].

A. HB Converter

Fig. 1(a) shows the HB converter topology. It is built with two transistors, with its antiparallel diodes, connected in series. This converter connects two voltages U_1 and U_2 by an inductor L. The HB converter is irreversible in voltage, but bidirectional in current.

The transfer functions that relate the two voltages and the two currents when the converter is working in the continuous conduction mode are

$$U_2 = D \cdot U_1 \tag{1}$$

$$I_1 = D \cdot I_2 \tag{2}$$

where U_1 and U_2 are the voltage levels in each side of the converter defined in Fig. 1(a), $0 \leq D \leq 1$ is the duty cycle, and I_1 and $I_L = I_2$ are the two currents in each side of the converter. As seen in Fig. 1(a), the condition $U_1 \geq U_2$ must be always satisfied for proper converter operation.

For a given input voltage U_1 and switching frequency F_s, the maximum inductor current ripple ΔI_L occurs for $D = 0.5$. Then, the value of the inductor can be calculated as [24]

$$L_{\mathrm{HB}} = \frac{U_1}{4\Delta I_L F_s}. \tag{3}$$

As can be seen in Fig. 1(b), the current waveform at voltage source U_1 has severe ripple.

The dc bus and the SCs can be connected either to U_1 or U_2. In regenerative braking applications, dc-bus voltage is supposed constant, while SC voltage changes in order to store or release energy.

In this paper, when the SCs are connected to U_1, the converter is said to work in the buck mode, because it reduces the SC voltage to the dc-bus voltage, and when connected to U_2, it is said that the converter works in the boost mode, because it elevates the SC voltage to the dc-bus voltage.

SCs are normally operated between rated voltage and half of the rated voltage because within this voltage range, they deliver 75% of the energy stored [8]. For constant power operation, SC current is lower, increasing efficiency.

As shown in Fig. 2(a), when working in the buck mode, the SCs are fully charged at $2U_{\mathrm{DC}}$. The initial converter duty cycle is 0.5, but as the SCs are discharged, its voltage decreases, and the duty cycle increases up to the maximum value of 1. In this discharge process, the inductor current is maintained constant to $I_{\mathrm{DC}} = \langle I_2 \rangle = \langle I_L \rangle$ when the power level at the dc bus is maintained constant.

As shown in Fig. 2(b), when working in the boost mode, the initial full charge voltage of the SCs is the same as the dc-bus voltage. When SCs are discharged, its voltage is reduced to half of the dc-bus voltage, and the duty cycle is also decreased down to 0.5. In this discharge process, the average inductor current $\langle I_L \rangle = \langle I_2 \rangle = \langle I_{\mathrm{SC}} \rangle$ will become twice when the power level at the dc bus is maintained constant compared to the buck mode.

Cascaded and modular multilevel dc/dc converters split the converter into smaller modules or cells, allowing multiple input and output voltage and current levels, and switching frequencies. Each module can be operated independently. In these topologies, redundancy in combination with hot-swap capability of modules can be achieved. When splitting the power sources, the energy management can be improved because it can be independent for each energy source [19]. However, in this paper, equal modules are supposed.

The cascaded and multilevel converters proposed here are the series connection of HB converters. Depending on where the SCs are connected and how the HB converters are arranged,

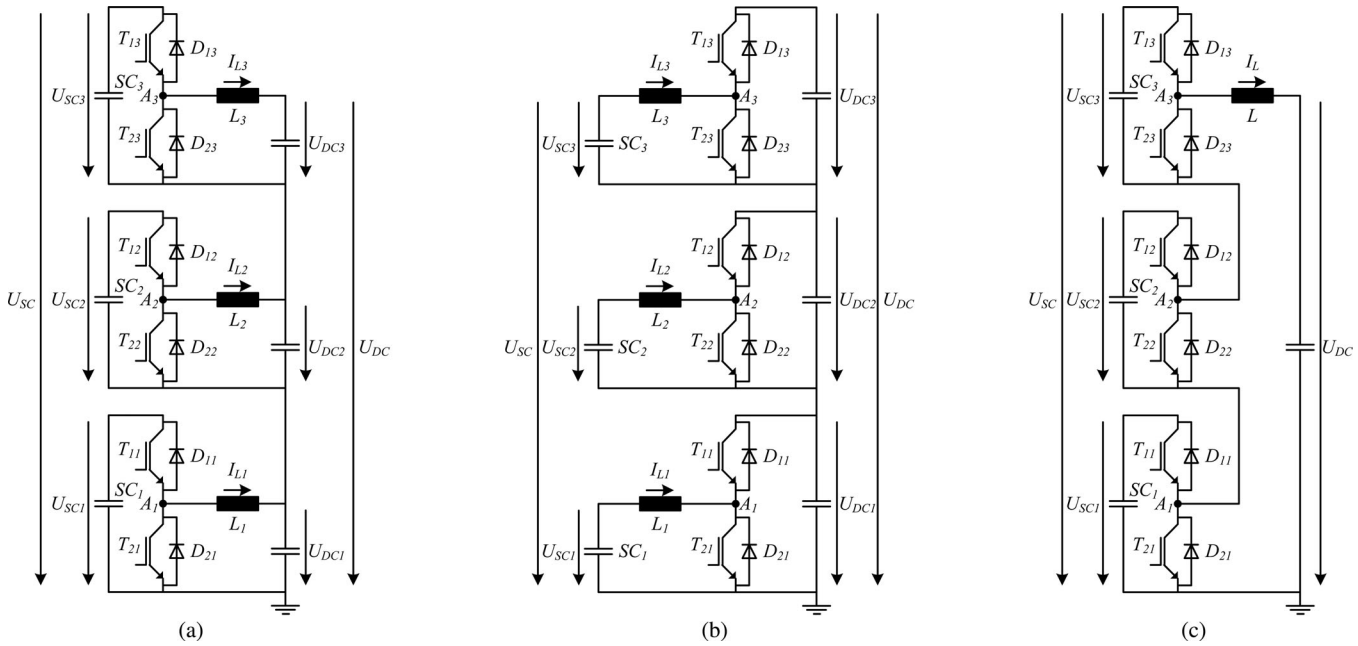

Fig. 3. Three-level example of the three topologies compared. (a) CBk. (b) CBt. (c) MMC.

three topologies are investigated and compared in this paper: cascaded buck (CBk), cascaded boost (CBt), and the modular multilevel dc/dc converter (MMC). These three topologies can be seen in Fig. 3(a)–(c), respectively, and are detailed in the following sections.

B. Cascaded Buck Converter (CBk)

The CBk can be seen in Fig. 3(a). It is built from the series connection of HB converters in the low-voltage side U_2, while the SCs are placed in the high-voltage side U_1 of the HB converter.

Because this topology works in the buck mode, when the SCs are fully charged $U_{\rm SCN} = 2U_{\rm DC}/N$, where N is the number of series-connected modules. The inductance value of each converter can be computed as

$$L_{{\rm CBk}N} = \frac{U_{DC}}{2\Delta I_L F_s N}. \tag{4}$$

As can be seen in (4), the inductor is split into several smaller inductors, but the total amount of energy stored in all the inductances is the same as for a unique converter with total voltage rating.

C. Cascaded Boost Converter (CBt)

The CBt can be seen in Fig. 3(b). It is made from the series connection of HB in the high-voltage side U_1, while the SCs are placed in the low-voltage side U_2.

Because this topology works in the boost mode, when SCs are half-charged $U_{\rm SC} = \frac{U_{\rm DCN}}{2} = U_{\rm DC}/\left(2N\right)$, the duty cycle is 0.5 and maximum inductor current ripple occurs. The inductance value of each converter can be computed as

$$L_{{\rm CBt}N} = \frac{U_{\rm DC}}{4\Delta I_L F_s N}. \tag{5}$$

As can be seen in (5), the inductance value can be one half that for the case of a CBk (assuming the same inductor current ripple), but to maintain power level, the inductor current level must be doubled. If we assume that the inductor current ripple percentage of maximum average inductor current is constant, the inductor value can be four times smaller than the CBk because the current is twice. Then, the inductor size and weight of two converters will be the same.

D. Modular Multilevel DC/DC Converter

The modular multilevel dc/dc converter is shown in Fig. 3(c). The converter is made from the series connection of HBs. It has only one inductor for the whole converter. That makes the converter as a unique converter, not the series connection of converters as in cascaded converters. MMCs are mainly used in HVDC systems because its modularity allows high voltage levels [25]. In the proposed converter, the application to HVDC systems can be as a energy storage system.

In the modular multilevel dc/dc converter proposed in this paper, the SCs are connected in the high-voltage side U_1. The output converter voltage U_2 is the addition of each output voltage $U_{\rm AN}$ that depends on the switching state of each HB and modulation strategy used. Each HB has a $U_{\rm SCN} = U_{\rm SC}/N$ voltage level.

Several modulation strategies exist for this type of converters [26]. In this paper, phase shifting modulation is used because it offers several advantages over others.

As can be seen in Fig. 4, using this modulation strategy, the triangular pulse-width-modulated (PWM) carriers are shifted $360^\circ/N$ with respect to the next HB. The frequency seen by the inductor is N times the HB switching frequency, $F_{\rm eq} = N \cdot F_s$, and the applied inductor voltage is only $U_{\rm SCN}$ [27].

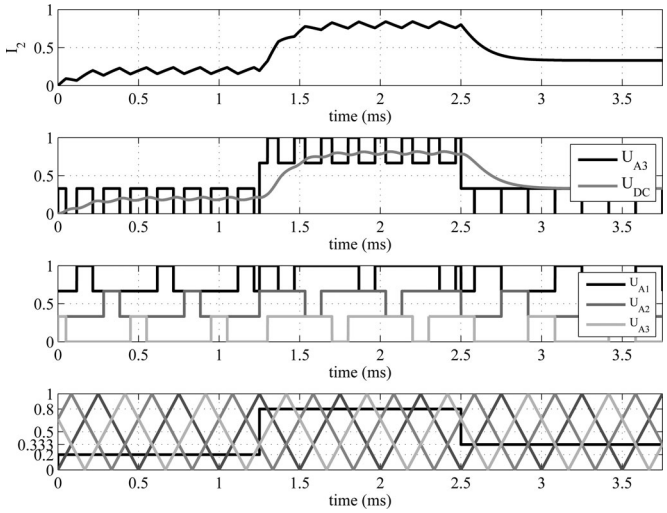

Fig. 4. Four-level modular multilevel dc/dc converter typical waveforms. For symbols, refer to Fig. 3.

These are the main benefits of using this modulation strategy for the modular multilevel dc/dc converter.

Because it is a buck-type converter, when the SCs are fully charged, $U_{\mathrm{SCN}} = 2U_{\mathrm{DC}}/N$. Then, the inductance $L_{\mathrm{MBk}N}$ can be computed as

$$L_{\mathrm{MBk}N} = \frac{U_{\mathrm{DC}}}{2\Delta I_2 F_s N^2}. \tag{6}$$

It has to be noted that the inductor value reduction depends on the square of the number of series-connected HBs.

E. SC Considerations: Input Filter

As said previously, SCs can be connected in the high-voltage side U_1 or in the low-voltage side U_2. But as can be seen in Fig. 1(b), when connected to the low-voltage side U_2, the inductor and SC current ripple is smaller compared with when connected to the high-voltage side U_1.

SCs cannot attenuate high-frequency currents. They behave as a resistor for frequencies above 100 Hz [28]. Therefore, when connected to the high-voltage side, filters must be installed [8]. *LC* filters are used because of low losses and simple design [28]. CBk and modular multilevel dc/dc converters need filters for SC current. Fig. 5 shows the *LC* filter used to filter input currents in SCs.

An attenuation of approximately -30 dB can be easily obtained with an L_f of 1% of the HB one-level converter inductor, and a filter capacitor C_f for a cutoff frequency five times smaller than the switching frequency [29].

When using filter in the SCs in the CBk and modular multilevel dc/dc converter, losses in SCs are reduced by a factor of D [29], but the inclusion of this filter can cause input disturbances to the controller [30].

F. Comparison of Different Topologies

In order to be able to know the optimal number of series-connected converters to decrease the size of the magnetic components, the total magnetic energy stored will be calculated for each proposed topology.

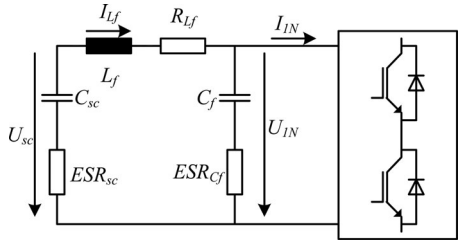

Fig. 5. SCs low-pass filter. U_{sc} is the variable voltage of the SC, L_f and C_f are the inductance and the capacitor filters, respectively, U_{1N} is the voltage of the cell, and I_{1N} is the cell input current. C_{sc} and $\mathrm{ESR}_{\mathrm{sc}}$ are the SC capacity and equivalent series resistance, respectively.

The base value for comparison will be the total magnetic energy stored in the one module cascaded buck topology

$$E_{\mathrm{CBk1}} = \frac{1}{2} L_{\mathrm{CBk1}} I_{\mathrm{DC}}^2. \tag{7}$$

1) CBk: From (4), the total energy stored plus the energy stored in the filter inductance is

$$E_{\mathrm{CBk}N} = \frac{1}{2} L_{\mathrm{CBk1}} I_{\mathrm{DC}}^2 N + 0.01 \frac{1}{2} L_{\mathrm{CBk1}} I_{\mathrm{DC}}^2 N \tag{8}$$

and, as $L_{\mathrm{CBk}N} = N L_{\mathrm{CBk1}}$, (8) can have the form

$$e_{\mathrm{CBk}} = \frac{E_{\mathrm{CBk}N}}{E_{\mathrm{CBk1}}} = 1 + 0.01N. \tag{9}$$

2) CBt: From (5), the total energy stored can be computed as

$$E_{\mathrm{CBt}N} = \frac{1}{2}\frac{1}{4} L_{\mathrm{CBk1}} \left(2I_{\mathrm{DC}}\right)^2 N = \frac{1}{2} L_{\mathrm{CBk1}} I_{\mathrm{DC}}^2 N. \tag{10}$$

Therefore, (10) can be rewritten as

$$e_{\mathrm{CBt}N} = \frac{E_{\mathrm{CBt}N}}{E_{\mathrm{CBk1}}} = 1. \tag{11}$$

3) Modular Multilevel DC/DC Converter: From (6), the total energy stored plus the energy stored in the filter inductance can be computed as

$$E_{\mathrm{MBk}N} = \frac{1}{2} L_{\mathrm{MBk}N} I_{\mathrm{DC}}^2 + 0.01 \frac{1}{2} L_{\mathrm{CBk1}} I_{\mathrm{DC}}^2 N \tag{12}$$

and, as $L_{\mathrm{MBk}N} = L_{\mathrm{CBK1}}/N^2$, (12) can be written as

$$e_{\mathrm{MBk}N} = \frac{E_{\mathrm{MBk}N}}{E_{\mathrm{CBk1}}} = \frac{1}{N^2} + 0.01N. \tag{13}$$

Fig. 6 shows the energy e for each topology as a function of the number of cascaded or series-connected HB converters. As can be seen, the minimum e is for the case of modular multilevel dc/dc converter with six series-connected converters, that is, a seven-level modular multilevel dc/dc converter. This is the proposed converter in this paper, and is depicted in Fig. 7.

G. Inductance Reduction Verification

The reduction of size and volume of the inductance needed by the modular multilevel dc/dc converter is compared to the

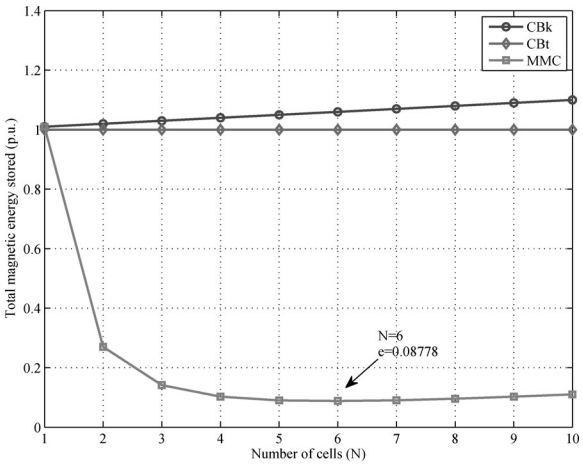

Fig. 6. Total magnetic energy stored as a function of the number of levels.

needed inductance for an HB converter. The inductor is designed here for the experimental setup parameters and conditions shown in Section IV and summarized in Table III.

The number of turns for a desired inductance value that do not saturate the magnetic core can be computed as

$$n = \frac{L \cdot I_{\rm sat}}{B_{\rm sat} \cdot A_e} \tag{14}$$

where L is the desired inductance value, $I_{\rm sat}$ is the desired saturation current, $B_{\rm sat}$ is the saturation flux density, and A_e is the cross-sectional area of the magnetic core.

The air gap to obtain the inductance value can be computed as

$$l_g = \mu_0 \frac{n^2 \cdot A_e}{L}. \tag{15}$$

With a maximum current ripple of 15%, the computed output inductance is 45 μH in the case of seven-level modular multilevel dc/dc converter and 1.26 mH in the case of a unique HB converter.

Table I summarizes the most important data for the inductor design. The selected core material is a 3C92 ferrite with a saturation flux density of $B_{\rm sat} = 375$ mT. Saturation current $I_{\rm sat}$ is fixed to 6 A. Current density J of 5 A/mm^2 and a nominal current of 5 A is assumed.

As can be seen in Table I, the RM10/ILP core solution for the modular multilevel dc/dc converter is 19 times smaller and 13 times lighter than the solution for the HB converter. This relation is almost the same as in the case of the magnetic energy stored, which is 11.4, as can be seen in Fig. 6.

These ratios are not equal because the cores are discrete components and the inductances have to be designed according to available cores.

III. Converter Control

The converter is aimed to store the regenerative braking energy in the SCs and release it when needed. This power flow

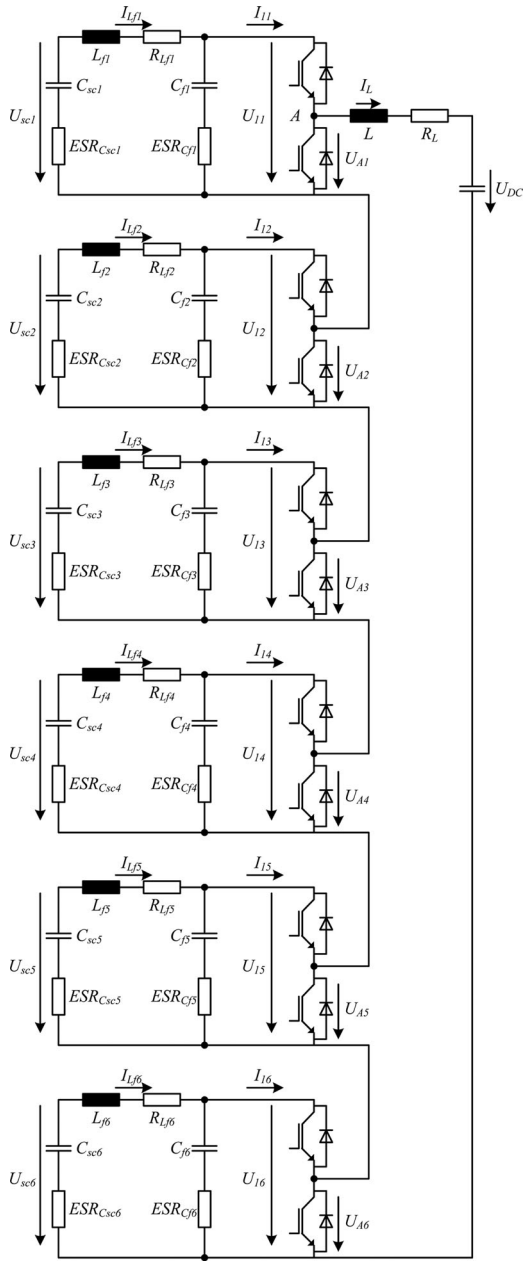

Fig. 7. Seven-level modular multilevel dc/dc converter. All the SC modules, with input filter and the six series-connected HBs, can be seen.

can be easily controlled by controlling the current in the output inductor I_L. But this reference level for output current is fixed by a higher level control system that is out of the scope of this paper.

Another control objective of the converter is to equalize the energy stored in the SCs. That can be done by controlling SC voltage to be the same value. Balancing is crucial to obtain constant current ripple at the output inductor.

From the I_L controller point of view, the modular multilevel dc/dc converter can be seen as a HB converter, as shown in Fig. 8. Common techniques can be used to design the controller G_c.

TABLE I
DESIGN PARAMETERS FOR THE INDUCTANCES

	core model	L (μH)	n	l_g (mm)	V (mm^3)	m_{Fe} (g)	m_{Cu} (g)	m_{tot} (g)
Half-bridge	E55/28/21	1260	58	1.18	81.670	216	60.2	276.2
Multilevel DC/DC	RM10/ILP	45	8	0.18	4.247	17	3.7	20.7

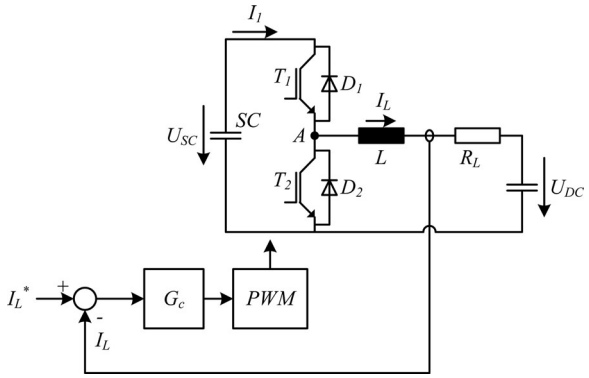

Fig. 8. Simplified diagram of the converter used for control purposes.

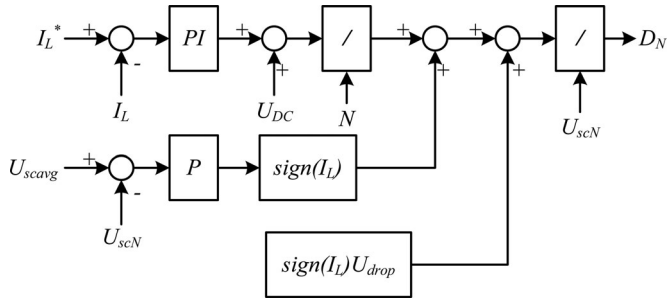

Fig. 9. Control scheme.

A. Current Control Loop

The system to be controlled is a first-order *RL* system that can be defined as

$$G_s(s) = \frac{\frac{1}{R_L}}{1 + s\frac{L}{R_L}}. \tag{16}$$

First-order systems can be controlled with zero steady-state error using a proportional-integral (PI) controller. Here, the controller is tuned using an indirect matrix converter method where K_p and K_i are selected as [31], [32]

$$K_p = \alpha \cdot L \tag{17}$$

$$K_i = \alpha \cdot R_L \tag{18}$$

where α is selected to fix the 10–90% rise time t_r as

$$t_r = \frac{\ln 9}{\alpha}. \tag{19}$$

B. SC Voltage-Balancing Loop

SC voltage balancing is crucial in order to store the maximum possible energy in SCs. Also, a shifted switching modulation strategy demands for equal voltages if a constant inductor current ripple is desired. Therefore, a voltage-balancing loop is a must in order to ensure correct converter operation.

The current loop outputs the average duty cycle of each of the series-connected HB, that is, the average duty cycle of the converter. In the proposed six-cell converter, there exist six degrees of freedom. These are the six different SC voltages, and these degrees of freedom can be used to balance SC voltages.

The reference voltage for the SC voltage-balancing loop cannot be set as a constant, because the voltage of each SC is changing in the charging–discharging process. The control objective is to maintain the same voltage level in each as they are charging or discharging. That means that the stored energy is the same in each SC, because the capacities are supposed to be equal.

This control objective can be accomplished comparing the individual SC voltage to the average of all SC voltages. In this case, the system to be controlled is just the voltage on an equivalent supercapacitor as

$$G_{sC}(s) = \frac{1}{sC_{\mathrm{SC}}}. \tag{20}$$

Here, just a P controller can be used. The Bode diagram of the transfer function is a straight line with -20 dB/decade that crosses the 0 dB at $\omega_0 = \frac{1}{C_{\mathrm{SC}}}$ and the controller adds some gain, moving up this line as

$$K_{p\mathrm{SC}} = 10^{\frac{-3}{20}} \frac{\omega_c}{\frac{1}{C_S C}} \tag{21}$$

where ω_c is the desired bandwidth of the closed-loop system. This bandwidth must be chosen low enough not to perturb the current loop and to limit SC currents when balancing SC voltages.

As can be seen in Fig. 9, the output of the balancing controller is added to the output of the current controller taking into consideration the current sense. With this compensation, the value of each SC will tend to the average value.

C. Semiconductor Voltage Drop Compensation

One of the main drawbacks of the modular multilevel dc/dc converter presented here is the large number of semiconductors connected in series. Each semiconductor, transistor or diode, has a voltage drop that can affect the performance of the control loop.

In order to obtain a good current response, the voltage drop in semiconductors must be compensated. Because of integral nature of the controller, the PI controller itself is able to compensate this disturbance, but better results can be obtained when the disturbance is compensated.

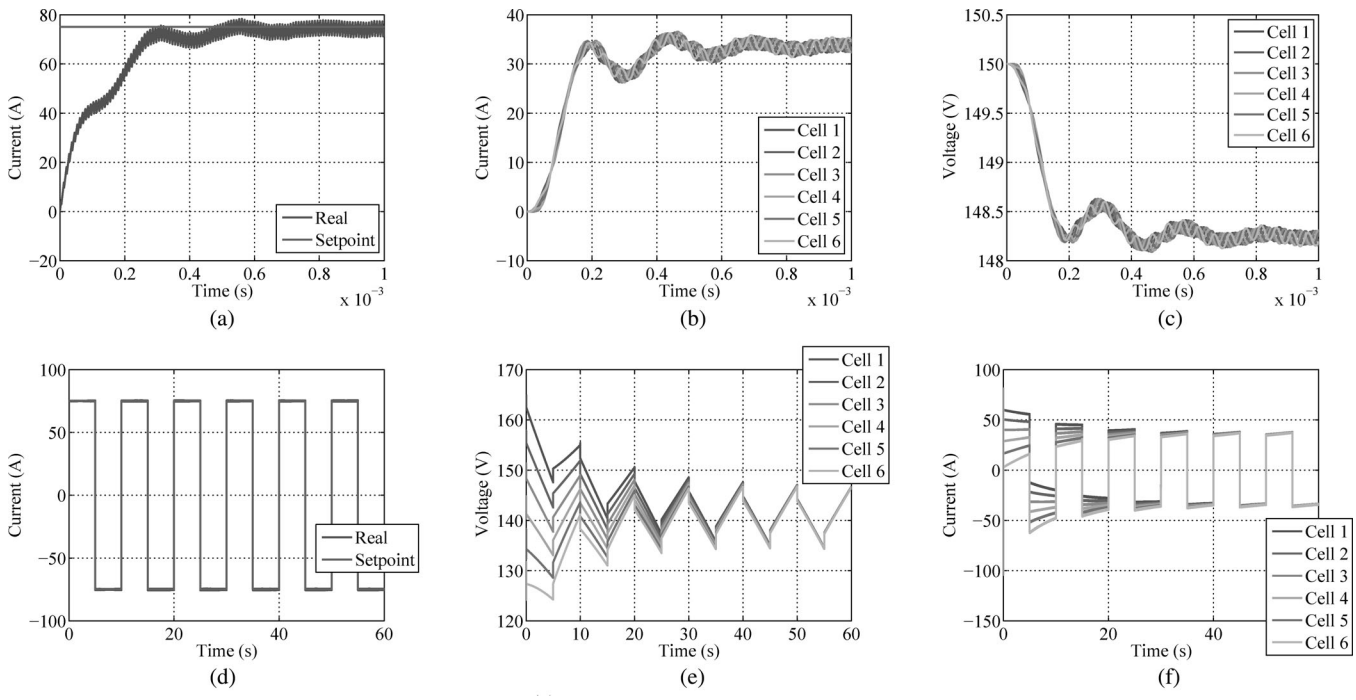

Fig. 10. Simulation results. (a) Output current response. (b) SC current response. (c) SC voltage response. (d) Charge and discharge output current. (e) SC voltage-balancing loop. (f) SC current balancing.

TABLE II
SIMULATION PARAMETERS

Parameter	Name	Value
F_s	Switching frequency	20 kHz
F_{ctrl}	Control execution frequency	120 kHz
U_1	Input voltage	900 V
U_2	Output voltage	400 V
C_{sc}	SC capacity	18.75 F
ESR_{sc}	SC Equivalent Series Resistance	60 mΩ
L	Output inductor inductance	41.67 μH
R_L	Output inductor resistance	14 mΩ
L_f	Filter inductor inductance	15 μH
R_{Lf}	Filter inductor resistance	5.7 mΩ
C_f	Filter capacitor capacity	150 μF
ESR_{Cf}	Filter capacitor ESR	1.9 mΩ
r_{on}	IGBT On resistance	1 mΩ
U_{drop}	IGBT voltage drop	1.5 V
t_r	Rise time (controller)	0.4 ms

This disturbance is compensated adding to the output of the current controller the semiconductor voltage drop as

$$D_{\text{drop}} = \text{sign}(I_2)\frac{U_{\text{drop}}}{U_{\text{sc}}}. \tag{22}$$

The complete control scheme can be seen in Fig. 9.

D. Simulation Results of the Proposed Converter and Control Scheme

The control scheme simulated and implemented in an experimental setup is depicted in Fig. 9. A model of the seven-level modular multilevel dc/dc converter shown in Fig. 7 has been implemented with MATLAB/Simulink software. The parameters of the simulated model are shown in Table II.

As can be seen in Fig. 10(a), the response of the controller to a current step of 75 A has a rising time approximately of 0.4 ms as designed. The low-frequency ripple current is due to the dynamics of the L_fC_f current SC filter [30]. If better dynamics are desired, the voltage of the HB input U_{1N} must be used to compute the desired duty cycle D instead of the SC voltage, as shown in Fig. 9. Fig. 10(b) and (c) shows the current and voltage at SCs, respectively. The initial voltage drop is due to SC internal resistance.

An average model of the seven-level modular multilevel dc/dc converter is implemented in MATLAB/Simulink to evaluate

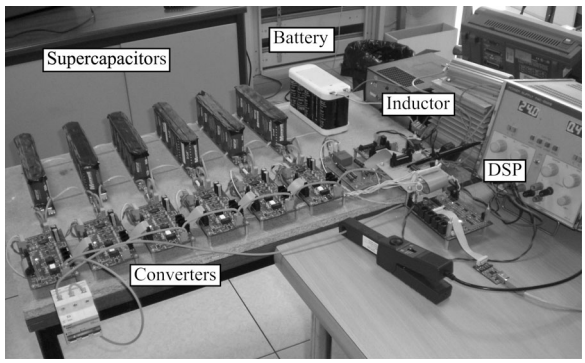

Fig. 11. Experimental setup. The blue cylinders are the SCs, and the green boards are the converters.

TABLE III
EXPERIMENTAL PARAMETERS

Parameter	Name	Unit
U_1	Input voltage	97.2 V
U_2	Output voltage	12 V
C_{sc}	SC capacity	58.3 F
ESR_{sc}	SC ESR	8.8 mΩ

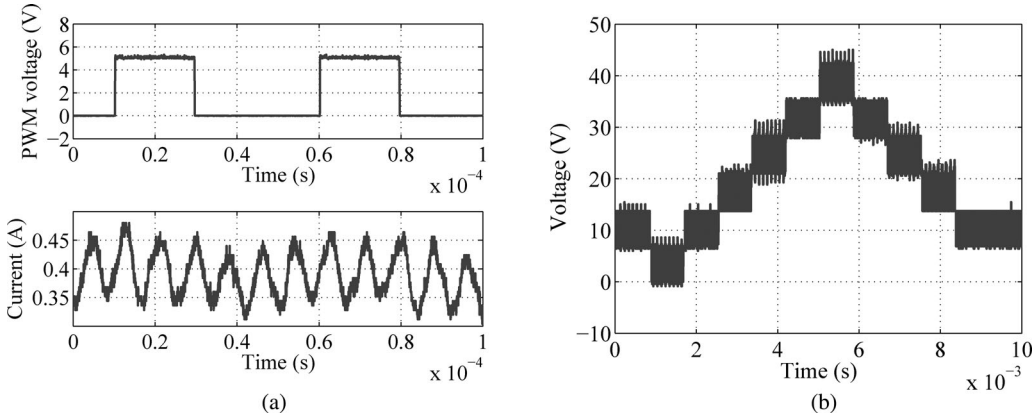

Fig. 12. Open-loop response of the proposed modular multilevel dc/dc converter. (a) PWM signal for one of the HBs and output current ripple. (b) Output converter voltage. It can be clearly seen the seven levels of the converter.

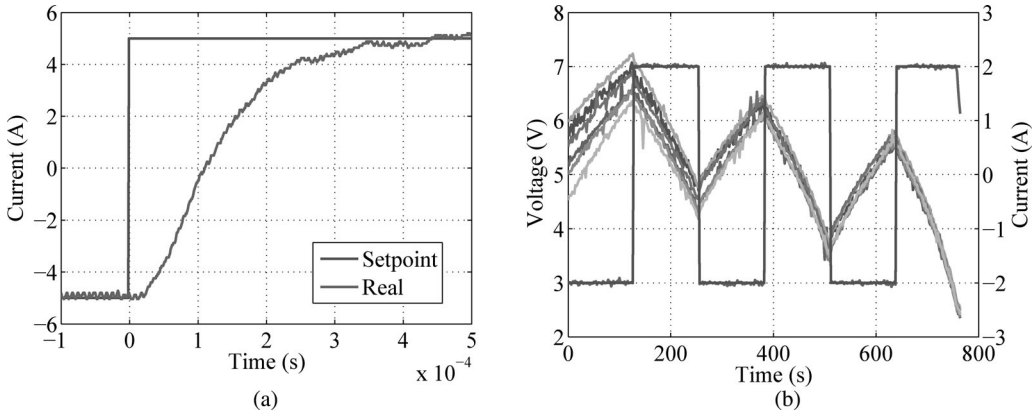

Fig. 13. Closed-loop experimental results for the modular multilevel dc/dc converter. (a) Dynamic response of the output current controller. (b) SC voltage-balancing loop response when applying output current reference steps from −2 to 2 A.

the performance of the SC balancing loop. As can be seen in Fig. 10(e), the SC initial voltage is different for each SC. Once the converter is activated, with current steps of ±75 A each 5 s [see Fig. 10(d)], the voltage-balancing loop tends to equalize the voltage at SCs. Because this voltage-balancing loop slightly modifies the duty cycle in each of the HBs, the current of each SC is different, as can be seen in Fig. 10(f).

IV. Experimental Results

The proposed converter and its control scheme have been implemented in an experimental setup shown in Fig. 11. It can be clearly seen the six SC modules, the six HB converters, including transistors, drivers, and voltage and current measurements needed, the DSP control board (on the right), the inductor, and the battery used to do the experiments. The parameters of the experimental test bed are shown in Table III.

The control algorithm has been implemented in a Texas Instruments DSP TMS320F2808 in C code. Inductor current is sampled at the switching frequency, 120 kHz. The current loop is also closed at 120 kHz. Because of lower bandwidth, SC voltage-balancing loop is implemented at 20 kHz.

Fig. 12 shows the converter behavior during open-loop operation. In Fig. 12(a), PWM signals for one of the six HBs are compared to output inductor current. It can be seen that the current has six times the switching frequency due to the modulation strategy used. Fig. 12(b) shows the seven levels of the converter when changing the duty cycle D from zero to one in a ramp.

Fig. 13 shows the response of the output current controller and the SC voltage-balancing loop. In Fig. 13(a), the current response can be seen when a reference step change is applied from −5 to 5 A. The change takes 0.4 ms as designed. Fig. 13(b) shows the response of the voltage-balancing loop. The SCs are precharged at different voltage levels from 3 to 6 V and then current steps from −2 to 2 A are applied to charge and discharge the SCs while the voltage-balancing loop equalizes voltages at SCs. As can be seen, the dynamic response of this loop is slow, but it must be noted that in steady-state operation of the converter, the SC voltages will be equal. This loop must ensure that these voltages are maintained equal during normal operation.

V. Conclusion

This paper has presented a modular multilevel dc/dc converter to be used in regenerative applications with SCs. The main objectives of reducing output inductor size and weight and achieving voltage balancing in SCs are accomplished.

A phase shift switching modulation strategy in modular multilevel dc/dc converters allows for lower voltage level and higher frequency voltage applied to the inductor, reducing its size and weight. Equal voltage module is a must in modular multilevel dc/dc converter to maintain current ripple when the phase shift switching modulation strategy is used. It is also needed to balance the stored energy in SCs. The voltage-balancing loop proposed in this paper balances the voltage even when SCs are charging or discharging.

All these features have been demonstrated in simulations and in an experimental setup.

ACKNOWLEDGMENT

The SC modules for the experimental setup have been generously provided by Maxwell Technologies SA, Rossens, Switzerland.

REFERENCES

[1] J. M. Miller, *Propulsion Systems for Hybrid Vehicle* (Renewable Energy Series), 2nd ed. Stevenage, U.K.: Institution of Engineering and Technology, 2010.

[2] A. Rufer and P. Barrade, "A supercapacitor-based energy-storage system for elevators with soft commutated interface," *IEEE Trans. Ind. Appl.*, vol. 38, no. 5, pp. 1151–1159, Sep.–Oct. 2002.

[3] L. Zhou, Z. Dong, S. Wang, and Z. Qi, "Design and analysis of a hybrid backup power system for a high-rise and high-speed elevator," in *Proc. IEEE/ASME Int. Conf. Mechtron. Embedded Syst. Appl.*, 2008, pp. 292–297.

[4] A. Rufer, "Energy storage for railway systems, energy recovery and vehicle autonomy in europe," in *Proc. Int. Power Electron. Conf.*, 2010, pp. 3124–3127.

[5] J. Larminie and J. Lowry, *Electric Vehicle Technology Explained*. New York: Wiley, 2003.

[6] J. Dixon, S. Bosch, C. Castillo, and M. Mura, "Ultracapacitors as unique energy storage for a city-car using five-level converter," in *Proc. 35th Annu. Conf. IEEE Ind. Electron.*, 2009, pp. 3854–3859.

[7] P. Thounthong and S. Rael, "The benefits of hybridization," *IEEE Ind. Electron. Mag.*, vol. 3, no. 3, pp. 25–37, Sep. 2009.

[8] J. M. Miller, *Ultracapacitor Application*, vol. 1, 1st ed. Stevenage, U.K.: Institution of Engineering and Technology, 2011.

[9] A. Xu, S. Xie, and X. Liu, "Dynamic voltage equalization for series-connected ultracapacitors in EV/HEV applications," *IEEE Trans. Veh. Technol.*, vol. 58, no. 8, pp. 3981–3987, Oct. 2009.

[10] X. Fang, N. Kutkut, J. Shen, and I. Batarseh, "Analysis of generalized parallel-series ultracapacitor shift circuits for energy storage systems," *Renewable Energy*, vol. 36, no. 10, pp. 2599–2604, Oct. 2011.

[11] (2012). [Online]. Available: http://koneika.com

[12] B. Destraz, Y. Louvrier, and A. Rufer, "High efficient interleaved multichannel dc/dc converter dedicated to mobile applications," in *Proc. 41st IEEE Ind. Appl. Soc. Annu. Meet. Ind. Appl. Conf.*, 2006, vol. 5, pp. 2518–2523.

[13] O. Garcia, P. Zumel, A. de Castro, and A. Cobos, "Automotive DC-DC bidirectional converter made with many interleaved buck stages," *IEEE Trans. Power Electron.*, vol. 21, no. 3, pp. 578–586, May 2006.

[14] S. Dwari and L. Parsa, "An efficient high-step-up interleaved DC-DC converter with a common active clamp," *IEEE Trans. Power Electron.*, vol. 26, no. 1, pp. 66–78, Jan. 2011.

[15] O. Hegazy, J. van Mierlo, and P. Lataire, "Analysis, modeling, and implementation of a multidevice interleaved DC/DC converter for fuel cell hybrid electric vehicles," *IEEE Trans. Power Electron.*, vol. 27, no. 11, pp. 4445–4458, Nov. 2012.

[16] F. Zhang, F. Z. Peng, and Z. Qian, "Study of the multilevel converters in DC-DC applications," in *Proc. IEEE 35th Annu. Power Electron. Spec. Conf. PESC 2004*, vol. 2, pp. 1702–1706.

[17] G. R. Walker and P. C. Sernia, "Cascaded DC-DC converter connection of photovoltaic modules," *IEEE Trans. Power Electron.*, vol. 19, no. 4, pp. 1130–1139, Jul. 2004.

[18] V. Vorperian, "Synthesis of medium voltage DC-to-DC converters from low-voltage, high-frequency PWM switching converters," *IEEE Trans. Power Electron.*, vol. 22, no. 5, pp. 1619–1635, Sep. 2007.

[19] W. Chen, X. Ruan, H. Yan, and C. K. Tse, "DC/DC conversion systems consisting of multiple converter modules: Stability, control, and experimental verifications," *IEEE Trans. Power Electron.*, vol. 24, no. 6, pp. 1463–1474, Jun. 2009.

[20] R. Giri, V. Choudhary, R. Ayyanar, and N. Mohan, "Common-duty-ratio control of input-series connected modular DC-DC converters with active input voltage and load-current sharing," *IEEE Trans. Ind. Appl.*, vol. 42, no. 4, pp. 1101–1111, Jul.–Aug. 2006.

[21] L. A. Tolbert, F. Z. Peng, T. Cunnyngham, and J. N. Chiasson, "Charge balance control schemes for cascade multilevel converter in hybrid electric vehicles," *IEEE Trans. Ind. Electron.*, vol. 49, no. 5, pp. 1058–1064, Oct. 2002.

[22] L. M. Tolbert, F. Z. Peng, and T. G. Habetler, "Multilevel inverters for electric vehicle applications," in *Proc. Power Electron. Transp.*, 1998, pp. 79–84.

[23] A. Nami, F. Zare, A. Ghosh, and F. Blaabjerg, "A hybrid cascade converter topology with series-connected symmetrical and asymmetrical diode-clamped h-bridge cells," *IEEE Trans. Power Electron.*, vol. 26, no. 1, pp. 51–65, Jan. 2011.

[24] P. Barrade, *Électronique de puissance: Métholodkogie et convertisseurs élémentaires*. Lausanne, Switzerland: Presses polytechniques et universitaires romandes, 2006.

[25] M. Guan and Z. Xu, "Modeling and control of a modular multilevel converter-based HVDC system under unbalanced grid conditions," *IEEE Trans. Power Electron.*, vol. 2, no. 12, pp. 4858–4867, Dec. 2012.

[26] J. Rodriguez, L. G. Franquelo, S. Kouro, J. I. Leon, R. C. Portillo, M. A. M. Prats, and M. A. Perez, "Multilevel converters: An enabling technology for high-power applications," *Proc. IEEE*, vol. 97, no. 11, pp. 1786–1817, Nov. 2009.

[27] M. Massot-Campos, D. Montesinos-Miracle, S. Galceran-Arellano, and A. Rufer, "Multilevel two quadrant DC/DC converter for regenerative braking in mobile applications," in *Proc. 14th Eur. Conf. Power Electron. Appl.*, 2011, pp. 1–10.

[28] S. Basu and T. M. Undeland, "Voltage and current ripple considerations for improving lifetime of ultra-capacitors used for energy buffer applications at converter inputs," in *Proc. 25th Annu. IEEE Appl. Power Electron. Conf. Expo.*, 2010, pp. 244–247.

[29] M. Massot-Campos. (2011). "Convertidor DC/DC multinivell de dos quadrants aplicat al frenat regeneratiu mitjançant supercondensadors per vehicles elèctrics o híbrids," Master's thesis, Escola Tècnica Superior d'Enginyeria Industrial de Barcelona, Barcelona, Spain [Online]. Available: http://hdl.handle.net/2099.1/13462

[30] P. Barrade, "Comportement dynamique des ensembles filtre-convertisseur" Ph.D. dissertation, Laboratoire d'Electrotechnique et d'Electronique Industrielle (LEEI), Institut National Polytechnique de Toulouse, Toulouse, France, 1997.

[31] J. Dong and C. B. Brosilow, "Design of robust multivariable PID controllers via IMC," in *Proc. Amer. Control Conf.*, 1997, vol. 5, pp. 3380–3384.

[32] D. E. Rivera, M. Morari, and S. Skogestad, "Internal model control. 4. PID controller design," *Ind. Eng. Chem. Process Des. Dev.*, vol. 25, pp. 252–265, 1986.

Daniel Montesinos-Miracle (S'01–M'08–SM'12) was born in Barcelona, Spain, in 1975. He received the M.Sc. degree in electrical engineering from the School of Industrial Engineering of Barcelona, Polytechnic University of Catalonia (UPC), Barcelona, Spain, in 2000, and the Ph.D. degree from UPC in 2008.

In 2001, he joined Salicru Electronics, S.A., Santa Maria de Palautordera, Spain, as a Research and Development Engineer. Since 2001, he has been involved in research at the Centre of Technological Innovation in Static Converters and Drives, UPC, as a Research Collaborator. In 2005, he becomes a Lecturer in the Department of Electrical Engineering, UPC, where since 2012, he has been an Associate Professor. His primary research interests include power electronics, drives, and green energy converters.

Miquel Massot-Campos was born in Mallorca, Spain, on September 21, 1988. He received the degree in industrial engineering from the School of Industrial Engineering of Barcelona, Technical University of Catalonia (UPC), Barcelona, Spain, in 2011. He is currently working toward the Ph.D. degree in underwater robotics in the Systems, Robotics and Vision Group, Balearic Islands University, Palma de Mallorca, Spain.

In 2009, he joined the Centre of Technological Innovation in Static Converters and Drives Research Group, UPC, where he did his master thesis. In April 2012, he joined Systems, Robotics and Vision Group, Balearic Islands University. His research interests include the fields linked with power electronics, renewable energy integration in power systems, industrial automation, computer vision, and robotics.

Joan Bergas-Jané (M'97–SM'10) was born in Manresa, Spain, in 1970. He received the B.S. degree in industrial engineering and the Ph.D. degree in engineering from the Universitat Politècnica de Catalunya, Barcelona, Spain, in 1992 and 2000, respectively.

Since 2002, he has been an Assistant Professor in the Department of Electrical Engineering, Universitat Politècnica de Catalunya. His research interest lies in the areas of power system quality, power electronics, and digital motor control.

Samuel Galceran-Arellano was born in Lleida, Spain, in 1971. He received the M.Sc. degree in electrical engineering and the Ph.D. degree from the Polytechnic University of Catalonia (UPC), Barcelona, Spain, in 1997 and 2002, respectively.

In 1997, he joined the Department of Electrical Engineering, UPC, as an Assistant Professor. He developed several projects for industry, and in 2001, he joined the Center of Technological Innovation in Static Converters and Drives (CITCEA-UPC), UPC, where he belongs to the CITCEA-UPC Directorate staff. His primary research interests include motor control and converters for power supplies and drives.

Alfred Rufer (M'95–SM'01–F'06) received the M.S. degree from the Ecole Polytechnique Fédéral de Lausanne (EPFL), Lausanne, Switzerland, in 1976.

In 1978, he joined ABB, Turgi, Switzerland, where he was involved in the fields of power electronics and control, such as high-power variable frequency converters for drives, and also a Group Leader involved with power electronics development beginning in 1985. In 1993, he became an Assistant Professor with EPFL, where since 1996, he has been a Full Professor and the Head of the Industrial Electronics Laboratory (LEI). LEI is active in power electronics used in energy conversion and energy storage and in the modeling and simulation of systems, including control strategies and control circuits. He has authored or coauthored many publications on power electronics and applications, such as for multilevel converters for different energy-storage systems. He is the holder of several patents.